35th Annual International Conference of the IEEE EMBS
Osaka, Japan, 3 - 7 July, 2013

Mitigate B_1^+ inhomogeneity by nonlinear gradients and RF shimming

Yi-Cheng Hsu, Ying-Hua Chu, I-Liang Chern, Riccardo Lattanzi, Teng-Yi Huang, and Fa-Hsuan Lin

Abstract—**High-field MRI has the challenge of inhomogeneous B_1^+ and consequently an inhomogeneous flip angle distribution. This causes spatially dependent contrast and makes clinical diagnosis difficult. Under the small flip angle approximation and using nonlinear spatial encoding magnetic fields (SEMs), we propose a method to remap the B_1^+ map into a lower dimension coordinate system. Combining with RF shimming method, a simple pulse sequence design using nonlinear SEMs can achieve a homogenous flip angle distribution efficiently. Using simulations, we demonstrate that combining RF shimming and spatially selective RF excitation using generalized SEMs (SAGS) using linear and quadratic SEMs in a multi-spoke *k*-space trajectory can mitigate the B_1^+ inhomogeneity at 7T efficiently without using parallel RF transmission.**

I. Introduction

High-field MRI offers a great promise to generate images with high signal-to-noise ratio (SNR). Yet major technical challenge is the inhomogeneous flip angle distribution when a volume RF coil is used for RF excitation [1]. This artifact is due to the deleterious interaction between the dielectric properties of the sample and the radio-frequency fields [2-4]. Consequently, an imaging object with the size approximating to the human head can have a spatially varying flip angle distribution, where typically a larger flip angle at the center of the field-of-view (FOV) and a smaller flip angle at the periphery of the FOV [5]. This causes images with a spatially dependent T_1 contrast, which makes clinical diagnosis difficult.

Different methods for mitigating B_1^+ inhomogeneity have been proposed. Dedicated volume radio-frequency (RF) coils have been designed [6-8]. Spatially selective RF excitation [9] can design RF and gradient waveforms in order to generate a more homogeneous flip angle distribution after considering the inhomogeneous B_1^+ generated by a volume coil [10]. Alternativley, it has been suggested that flip angle distribution can become more homogeneous by using simultaneous RF excitation from multiple RF coils, including the RF shimming [11-15] and transmit SENSE [16, 17] methods. However, the challenges of parallel RF transmission method include the complexity of the RF electronics and coil construction in order to achieve simultaneous excitation, the necessity of accurate estimates of phases and amplitudes of the B_1^+ maps for each RF coil, and the specific absorption rate (SAR) management [18]. It has been also suggested that a more homogeneous image intensity can be obtained after appropriately combining images of different modes of a volume coil [19]. However, this method designed to improve the image intensity inhomogeneity rather than to reduce the flip angle inhomogeneity.

Recently, it has been demonstrated that nonlinear spatial magnetic fields (SEMs) can be used in MRI spatial encoding in order to improve spatiotemporal resolution [20, 21]. Preliminary studies using quadratic nonlinear SEMs for RF excitation [22, 23] and small FOV imaging have also been reported. Under the small flip angle approximation, a formulation describing the spatial distribution of the flip angle when RF pulse is transmitted with time-varying linear and nonlinear SEMs has been described before . Furthermore, methods of using linear and quadratic SEMs to compensate B_1^+ inhomogeneity have been proposed. Specifically, parallel RF transmission can be combined with higher spatial frequency encoding at the periphery of the FOV generated by a quadratic SEM to reduce flip angle inhomogeneity . Alternatively, driving linear and quadratic SEMs between two excitation pulses can generate spatially dependent transverse magnetization phase, which can counteract the inhomogeneous B_1^+ and consequently leads to more homogeneous flip angle distribution [24].

Here, under the small flip angle approximation [9], we propose a method to remap the B_1^+ map into a lower dimension coordinate system and chose corresponding RF shimming coil coefficients. Under the condition that the iso-intensity contours of the SEMs are similar to the iso-intensity contours of B_1^+, this remapping has the advantage of achieving a homogenous flip angle distribution efficiently by a simple pulse sequence design using time-varying linear and nonlinear SEMs. Importantly, we propose that by using the RF shimming method, this condition is much improved compared to the case where no RF shimming is used. Using simulations based the electromagnetics at 7T, we compare our method with the method of "tailored excitation" using nonlinear B_0-shim coils and a two-spoke trajectory [24]. Results demonstrate that the spatially selective RF excitation using generalized SEMs (SAGS) together with RF shimming

* Resrach supported by National Science Council, Taiwan (NSC 101-2628-B-002-005-MY3, NSC 100-2325-B-002-046), Ministry of Economic Affairs, Taiwan (100-EC-17-A-19-S1-175), National Health Research Institute, Taiwan (NHRI-EX102-10247EI), and the Academy of Finland (the FiDiPro program).

Yi-Cheng Hsu is with the Department of Mathematics, National Taiwan University, Taipei, Taiwan (phone: 886-2-33669702; fax: 886-2-33665268; e-mail: D96221003@ntu.edu.tw).

Ying-Hua Chu is with the Institute of Biomedical Engineering, National Taiwan University, Taipei, Taiwan (e-mail: d99548004@ntu.edu.tw).

I-Liang Chern is with the Department of Mathematics, National Taiwan University, Taipei, Taiwan (e-mail: chern@math.ntu.edu.tw).

Riccardo Lattanzi is with the Center for Biomedical Imaging, Department of Radiology, New York University Medical Center, New York, New York (e-mail: Riccardo.Lattanzi@nyumc.org).

Teng-Yi Huang is with the Department of Electrical Engineering, National Taiwan University of Science and Technology, Taipei, Taiwan(e-mail: tyhuang@ee.ntust.edu.tw).

Fa-Hsuan Lin is with the Institute of Biomedical Engineering, National Taiwan University, Taipei, Taiwan (e-mail: fhlin@ntu.edu.tw).

can achieve a homogeneous flip angle distribution ***without*** parallel RF transmission.

II. THEORY

A. Small flip angle approximation using nonlinear SEMs with inhomogeneous B_1^+

For an MRI system with n distinct configurations of SEMs during RF excitation, we use a dimensionless variable $\mathbf{f}(\mathbf{r})=[f_1(\mathbf{r}), \ldots, f_n(\mathbf{r})]$ to describe the spatial distributions of the z-components of these SEMs. To facilitate the description of the arbitrary spatial distribution of $\mathbf{f}(\mathbf{r})$, we define the maximal and the minimal values among all components of $\mathbf{f}(\mathbf{r})$ within the imaging object are 1 and 0 respectively. We use $\mathbf{g}(t)=[g_1(t)\ldots g_n(t)]$ to describe the instantaneous strength of each individual SEM in a physical unit of magnetic field strength. Accordingly, each component of $\mathbf{g}(t)$ clearly defines the instantaneous difference between the minimal and maximal z-component of the magnetic field generated by each SEM within the imaging objects. The instantaneous additional z-component of the magnetic field at location $\mathbf{r}$ is thus the inner product $\mathbf{g}(t)\cdot\mathbf{f}(\mathbf{r})$. Under small angle approximation [9], the transverse magnetization $M_{xy}(\mathbf{r})$ by the end of an RF pulse with duration T is:

$$\begin{aligned} M_{xy}(\mathbf{r}) &= j\gamma \int_0^T \frac{B_1(\mathbf{r},t)}{|\mathbf{k}'(t)|}\exp[j2\pi\mathbf{f}(\mathbf{r})\cdot\mathbf{k}(t)]\,|k'(t)|\,dt \\ \mathbf{k}'(t) &= \frac{d}{dt}\mathbf{k}(t) = -\gamma\mathbf{g}(t) \\ \mathbf{k}(t) &= [k_1(t), \cdots, k_n(t)] = \gamma\int_t^T \mathbf{g}(s)\,ds \end{aligned} \tag{1}$$

Note that the notation $\boldsymbol{k}$(t) in this study is different from that in conventional MRI [9]. We chose $\mathbf{k}(t)$ to express the maximal phase difference of the transverse magnetization precession within the imaging object at time instant t.

Since a k-space trajectory has the one-to-one correspondence between $\mathbf{k}(t)$ and t, we omit the t argument in $\mathbf{k}(t)$ and use $\mathbf{k}$ in the following. Additionally, we use a delta function $s(\mathbf{k})$ to describe the k-space trajectory.

Since $B_1(\mathbf{r},t)$ is spatiotemporally separable, we choose $B_1(\mathbf{r},t) = B_1(\mathbf{r}) \times B_1(t)$, where $B_1(t)$ is a waveform of the RF field in a physical unit of magnetic field strength, and $B_1(\mathbf{r})$ is a spatial distribution of the ratio between $B_1(\mathbf{r},t)$ and $B_1(t)$.

The spatial distribution of the transverse magnetization $M_{xy}(\mathbf{r})$, RF pulse waveform $B_1(t)$, and temporal integral of SEMs (linear/nonlinear MRI gradients) over time are related to each to other by an inverse Fourier transform [9]:

$$\begin{aligned} M_{xy}(\mathbf{r}) &= \int_K W(\mathbf{k})B_1(\mathbf{r})\exp[j2\pi\mathbf{f}(\mathbf{r})\cdot\mathbf{k}]s(\mathbf{k})\,d\mathbf{k} \\ W(\mathbf{k}) &= W(\mathbf{k}(t)) = \frac{j\gamma B_1(t)}{|\mathbf{k}'(t)|} \end{aligned} \tag{2}$$

B. Spoke trajectory for slice selection

A spoke trajectory $s(\mathbf{k})$ can be parameterized by k_z and $\mathbf{k}_f$: $s(\mathbf{k}) = s(k_z, \mathbf{k}_f)$, where k_z indicates the k-space coordinate determined by the linear Z SEM and $\mathbf{k}_f$ indicates the k-space coordinates determined by $\mathbf{f}(\mathbf{r})=[f_1(\mathbf{r}), \ldots, f_n(\mathbf{r})]$ SEMs. For simplicity we consider only exciting the central slice ($z = 0$; $\mathbf{r} = [x\ y]^T$). Each spoke at $\mathbf{k}_f$ can be described as a product between its waveform $W_z(k_z)$ and a complex valued weighting $W_F(\mathbf{k}_f)$: $W(k_z, \mathbf{k}_f) = W_z(k_z) \times W_F(\mathbf{k}_f)$. $W_z(k_z)$ typically has a SINC or Gaussian waveform such that $\int_{K_z} W_Z(k_z)\,dk_z = 1$, and $W_F(\mathbf{k}_f)$ determines the magnitude and the phase of the slice selective pulse. It should be noted that the integral in (2) can be described by a summation of integrations, each of which corresponds to one spoke, because $W(k_z, \mathbf{k}_f)= 0$ between spokes. Accordingly, (2) in a spoke trajectory becomes

$$\begin{aligned} M_{xy}(\mathbf{r}) &= B_1(\mathbf{r})\sum_{spokes} W_F(\mathbf{k}_f)\exp[2\pi j\mathbf{k}_f\cdot\mathbf{f}(\mathbf{r})]\times\int_{K_z} W_Z(k_z)\exp[2\pi jk_z z]dk_z, \\ M_{xy}(x,y) &= B_1(x,y)\sum_{spokes} W_F(\mathbf{k}_f)\exp[2\pi j\mathbf{k}_f\cdot\mathbf{f}(x,y)] \end{aligned} \tag{3}$$

where $M_{xy}(x,y)$ is the excited transverse magnetization at $z = 0$ plane.

C. The k-space trajectory dimension reduction using nonlinear SEMs

When both linear X and Y SEMs are used, (3) shows that $W_F(\mathbf{k}_f) = W_F(k_x, k_y)$ is the 2D discrete Fourier transform coefficient of $M_{xy}(x,y)/B_1(x,y)$. Suppose that we aim to achieve a target transverse magnetization distribution $M_{xy}(x,y)$ subject to the B_1^+ field $B_1(\mathbf{r}) = B_1(x, y)$ at $z =0$. If $M_{xy}(x,y)/B_1(x,y)$ can be parameterized by $\mathbf{f}(x,y)$, then (3) becomes

$$\begin{aligned} M_{xy}(x,y)/B_1(x,y) &= \tilde{M}_{xy}(\mathbf{f}(x,y)) \\ &= \sum_{spokes} W_F(\mathbf{k}_f)\exp[2\pi j\mathbf{k}_f\cdot\mathbf{f}(x,y)] \end{aligned} \tag{4}$$

This shows that the $W_F(\mathbf{k}_f)$ is the discrete Fourier transform coefficient of $\tilde{M}_{xy}(\mathbf{f}(x,y))$ The dimension of this discrete Fourier transform depends on the dimension of $\mathbf{f}(x,y)$. Using nonlinear SEM can be advantageous if there is an one-dimensional $f(x,y)$ such that

$$M_{xy}(x,y)/B_{1r}(x,y) \cup \tilde{M}(f(x,y)) \tag{5}$$

Then (4) becomes

$$M_{xy}(\mathbf{r}) = \tilde{M}_{xy}(f(x,y)) = \sum_{spokes} W_F(k_f)\exp[2\pi jk_f f(x,y)] \tag{6}$$

$W_F(\mathbf{k}_f)$ is the 1D discrete Fourier transform coefficient of $\tilde{M}(f(x,y))$. Reducing the dimension of the discrete Fourier transform from 2D to 1D implies that a shorter k-space trajectory can be used to achieve the similar distribution of the transverse magnetization.

D. Use RF shimming and nonlinear SEMs to achieve B_1^+ remapping

We approximate the desired $M_{xy}(x,y)/B_1(x,y)=M_{xy}/B_1(x,y)$ by a distribution consisting of a linear combination of cosine and sine harmonics: $\tilde{M}(f) = \sum_{l=0}^{L}\beta_l\cos(lf) + \sum_{l=1}^{L}\alpha_l\sin(lf)$, where α_i, β_i are the coefficients for harmonic and up to L harmonics are used in the approximation. Since we use quadratic SEMs in this study, f is quadratic function to be determined, therefore $f = ax^2 + by^2 + cxy + dx + ey + g$. Realistically β_i were estimated using a gradient decent method with the initial guess estimated by using only the first harmonic: $\tilde{M}_0(x,y) - \mu_1\cos(f)$, b1 was chosen as the maximum value of

$M_{xy}/B_1(x,y)$, and consequently the coefficient of each polynomial of f can be uniquely estimated by the least square fitting of $\arccos(M_{xy}/B_1(x,y))$. In RF shimming, $B_1(x,y) = s_i B_1^i(x,y)$ and in order to find the most suitable remapping coordinate, we can optimize the cost function:

$$\min_{a,b,c,d,e,g,\beta_l,\alpha_l,s_i} \| \sum_{i=1}^{I} s_i B_1^i(x,y) \sum_{l=0}^{L} (\beta_l \cos(lf) + \alpha_l \sin(lf)) - M_{xy} \|_2 \quad (7)$$

To optimize this function we first use gradient decent for parameters (a, b, c, d, e, g) then find the linear regression solution for (β_l, α_l) and s_i respectively. $f(x,y)$ was found by linearly scaling the fitted quadratic polynomial (7) such that its minimum and the maximum are 0 and 1 within the imaging object, respectively.

E. Design flip angle distribution using arbitrary SEMs using a spoke trajectory

When (5) is satisfied, the next step is to design the location k_f and the strength $W_F(k_f)$ using Eq. (6). In general, $\tilde{M}(f(x,y))$ can be approximated accurately by sufficient spokes. However since $\tilde{M}(f(x,y))$ is typically spatially smooth, it may be more efficient using irregularly spaced spokes in order to achieve the approximation in Eq. (6) with ony a few spokes. This idea is similar to the fast-k_z method, which uses spokes near the center of the k-space to approximate a quadratic transverse magnetization distribution. In practice, we propose using irregularly spaced spokes, whose strengths $W_F(k_f)$ can be estimated by the least squares criterion (3) and locations can be exhaustively sought over a set of candidate locations.

III. METHOD

A. B_1^+ simulation

Twenty B_1^+ maps for twenty RF coils uniformly distributed over a sphere phantom with 15cm radius were simulated using Multipole expansion [25]. The FOV is a transverse square section through the center of the sphere, with the side length equal to the sphere's diameter (image matrix = 32 X 32 voxels). The dielectric constant $\varepsilon = 52$ and the conductivity $\sigma = 0.55$. (1/Ω m)

B. RF shimming and RF shimming for B_1^+ remapping

The coefficient s_i for RF shimming without B_1^+ remapping were calculated by iteratively updating the target B_1^+ phase by the phase in the cost function after each optimization steps. The same procedure was applied with combined B_1^+ remapping with RF shimming (Eq, (7)). To evaluate the result of remapping, we plot the distribution between $f(x,y)$ and normalized $M_{xy}/B_1(x,y)$, which was linearly scaled $M_{xy}/B_1(x,y)$ such that the maximum = 1. Ideally this distribution should form a curve, which was estimated by fitting all points by a 10^{th}-order polynomial.

C. Comparison on relative RF power and $|M_{xy}|$ homogeneity between 1-pulse with RF shimming, SAGS with RF shimming, and two-pulse "tailored-excitation" methods

For comparison, we also calculated the $|M_{xy}|$ distributions with desired 30 degree flip angle generated by 1) one spoke using only linear z SEM with RF shimming, 2) a two-spoke "tailored-excitation" trajectory using both linear and quadratic with RF shimming alone and with combined RF shimming and B_1^+ remapping. Note that the two-spoke "tailored excitation" method can tune the amplitudes of two spokes; we used the minimal required amplitude. For the proposed SAGS method,we used 4 spokes.

The performance of $|B_1^+|$ homogeneity improvement was evaluated by the relative standard deviation

$$\sigma = \text{std}(|M_{xy}|)/\text{mean}(|M_{xy}|), \quad (8)$$

where std(•) and mean(•) denote taking the standard deviation and the mean respectively.

IV. RESULTS

A. B_1^+ of RF shimming and RF shimming for B_1^+ remapping

Figure 1 shows the B_1^+ distribution after RF shimming alone and after combining RF shimming and B_1^+ remapping. We observed that the result of RF shimming and B_1^+ remapping is more inhomogeneous, but its iso-intensity contour matches better to the iso-intensity contour of quadratic function. This is demonsrated in Figure 2, where plots between $M_{xy}/B_1(x,y)$ and $f(x,y)$ using RF shimming and B_1^+ remapping forms a dense distribution.

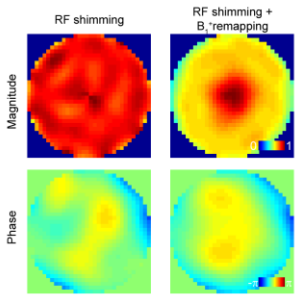

Figure 1 The B_1^+ magnitude and phase after RF shimming (Left) and after RF shimming with B_1^+ remapping.

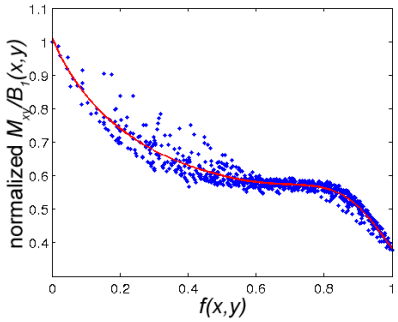

Figure 2 The $M_{xy}/B_1(x,y)$ - $f(x,y)$ plot. Blue dots represent the normalized empirical $M_{xy}/B_1(x,y)$ and calculated $f(x,y)$. The red solid curve represents the least squares error fitting to blue dots

B. Comparison on relative RF power and $|M_{xy}|$ homogeneity between 1-pulse with RF shimming, SAGS with RF shimming, and two-pulse "tailored-excitation" methods

Figure 3 shows the results using 1 pulse with RF shimming alone (Figure 3A) with σ=5.47% , and two spokes "tailored excitation" with RF shimming alone σ=5.42% (Figure 3B) which only has marginal improvement since the variation of B_1^+ does not match a quadratic function. Two spokes "tailored excitation" with RF shimming and B_1^+ remapping has σ=6.21%. However, SAGS using RF shimming and B_1^+

remapping can achieve the most homogeneous flip angle distribution (σ=2.57%).

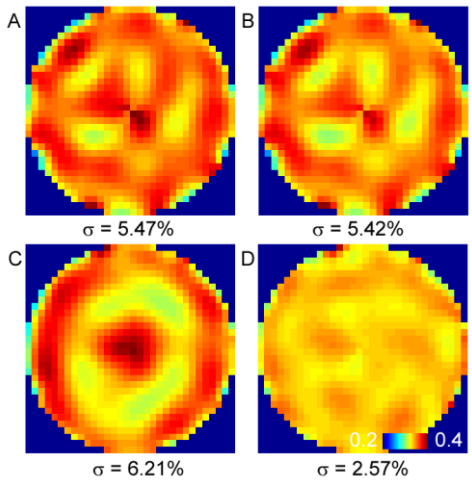

Figure 3 The simulated $|M_{xy}|$ using (A) RF shimming and one pulse (B) RF shimming and two-spokes "tailored excitation" (C) RF shimming for B_1^+ remapping and two-spokes "tailored excitation" (D) RF shimming for B_1^+ remapping and SAGS. σ is the relative standard deviation of $|M_{xy}|$.

V. Conclusion

Combining RF shimming and B_1^+ remapping, SAGS using a quadratic SEM can achieve a more homogeneous flip angle distribution than using RF shimming along or the two spokes "tailored excitation" method. We demonstrate that our method is an efficient method of achieving a homogeneous flip angle distribution by combining RF shimming and nonlinear SEMs without using parallel RF transmission.

References

[1]P. A. Bottomley and E. R. Andrew, "RF magnetic field penetration, phase shift and power dissipation in biological tissue: implications for NMR imaging," *Phys Med Biol,* vol. 23, pp. 630-43, Jul 1978.

[2]C. M. Collins, W. Liu, W. Schreiber, Q. X. Yang, and M. B. Smith, "Central brightening due to constructive interference with, without, and despite dielectric resonance," *J Magn Reson Imaging,* vol. 21, pp. 192-6, Feb 2005.

[3]P. F. Van de Moortele, C. Akgun, G. Adriany, S. Moeller, J. Ritter, C. M. Collins, *et al.*, "B(1) destructive interferences and spatial phase patterns at 7 T with a head transceiver array coil," *Magn Reson Med,* vol. 54, pp. 1503-18, Dec 2005.

[4]J. T. Vaughan, M. Garwood, C. M. Collins, W. Liu, L. DelaBarre, G. Adriany, *et al.*, "7T vs. 4T: RF power, homogeneity, and signal-to-noise comparison in head images," *Magnetic Resonance in Medicine,* vol. 46, pp. 24-30, Jul 2001.

[5]J. T. Vaughan, M. Garwood, C. M. Collins, W. Liu, L. DelaBarre, G. Adriany, *et al.*, "7T vs. 4T: RF power, homogeneity, and signal-to-noise comparison in head images," *Magn Reson Med,* vol. 46, pp. 24-30, Jul 2001.

[6]D. C. Alsop, T. J. Connick, and G. Mizsei, "A spiral volume coil for improved RF field homogeneity at high static magnetic field strength," *Magn Reson Med,* vol. 40, pp. 49-54, Jul 1998.

[7]J. T. Vaughan, G. Adriany, C. J. Snyder, J. Tian, T. Thiel, L. Bolinger, *et al.*, "Efficient high-frequency body coil for high-field MRI," *Magn Reson Med,* vol. 52, pp. 851-9, Oct 2004.

[8]G. Adriany, P. F. Van de Moortele, J. Ritter, S. Moeller, E. J. Auerbach, C. Akgun, *et al.*, "A geometrically adjustable 16-channel transmit/receive transmission line array for improved RF efficiency and parallel imaging performance at 7 Tesla," *Magn Reson Med,* vol. 59, pp. 590-7, Mar 2008.

[9]J. M. Pauly, D. G. Nishimura, and A. Macovski, "A k-space analysis of small-tip-angle excitation," *Journal of Magnetic Resonance,* vol. 81, pp. 43-56, 1989.

[10] S. Saekho, C. Y. Yip, D. C. Noll, F. E. Boada, and V. A. Stenger, "Fast-kz three-dimensional tailored radiofrequency pulse for reduced B1 inhomogeneity," *Magn Reson Med,* vol. 55, pp. 719-24, Apr 2006.

[11] T. S. Ibrahim, R. Lee, B. A. Baertlein, A. M. Abduljalil, H. Zhu, and P. M. Robitaille, "Effect of RF coil excitation on field inhomogeneity at ultra high fields: a field optimized TEM resonator," *Magn Reson Imaging,* vol. 19, pp. 1339-47, Dec 2001.

[12] W. Mao, M. B. Smith, and C. M. Collins, "Exploring the limits of RF shimming for high-field MRI of the human head," *Magn Reson Med,* vol. 56, pp. 918-22, Oct 2006.

[13] C. M. Collins, W. Liu, B. J. Swift, and M. B. Smith, "Combination of optimized transmit arrays and some receive array reconstruction methods can yield homogeneous images at very high frequencies," *Magn Reson Med,* vol. 54, pp. 1327-32, Dec 2005.

[14] T. Vaughan, L. DelaBarre, C. Snyder, J. Tian, C. Akgun, D. Shrivastava, *et al.*, "9.4T human MRI: preliminary results," *Magn Reson Med,* vol. 56, pp. 1274-82, Dec 2006.

[15] G. J. Metzger, C. Snyder, C. Akgun, T. Vaughan, K. Ugurbil, and P. F. Van de Moortele, "Local B1+ shimming for prostate imaging with transceiver arrays at 7T based on subject-dependent transmit phase measurements," *Magn Reson Med,* vol. 59, pp. 396-409, Feb 2008.

[16] U. Katscher, P. Bornert, C. Leussler, and J. S. van den Brink, "Transmit SENSE," *Magnetic Resonance in Medicine,* vol. 49, pp. 144-150, Jan 2003.

[17] W. Grissom, C. Y. Yip, Z. Zhang, V. A. Stenger, J. A. Fessler, and D. C. Noll, "Spatial domain method for the design of RF pulses in multicoil parallel excitation," *Magn Reson Med,* vol. 56, pp. 620-9, Sep 2006.

[18] R. Lattanzi, D. K. Sodickson, A. K. Grant, and Y. Zhu, "Electrodynamic constraints on homogeneity and radiofrequency power deposition in multiple coil excitations," *Magn Reson Med,* vol. 61, pp. 315-34, Feb 2009.

[19] S. Orzada, S. Maderwald, B. A. Poser, A. K. Bitz, H. H. Quick, and M. E. Ladd, "RF excitation using time interleaved acquisition of modes (TIAMO) to address B1 inhomogeneity in high-field MRI," *Magn Reson Med,* vol. 64, pp. 327-33, Aug 2010.

[20] J. P. Stockmann, P. A. Ciris, G. Galiana, L. Tam, and R. T. Constable, "O-space imaging: Highly efficient parallel imaging using second-order nonlinear fields as encoding gradients with no phase encoding," *Magn Reson Med,* vol. 64, pp. 447-56, Aug 2010.

[21] J. Hennig, A. M. Welz, G. Schultz, J. Korvink, Z. Liu, O. Speck, *et al.*, "Parallel imaging in non-bijective, curvilinear magnetic field gradients: a concept study," *MAGMA,* vol. 21, pp. 5-14, Mar 2008.

[22] C. Ma, D. Xu, K. F. King, and Z. P. Liang, "Reduced field-of-view excitation using second-order gradients and spatial-spectral radiofrequency pulses," *Magn Reson Med,* Apr 5 doi: 10.1002/mrm.24259.

[23] E. Kopanoglu, U. Yilmaz, Y. Gokhalk, and E. Atalar, "Specific absorption rate reduction using nonlinear gradient fields," *Magn Reson Med,* Sep 17 2012.

[24] Q. Duan, P. van Gelderen, and J. Duyn, "Tailored excitation using nonlinear B0-shims," *Magnetic Resonance in Medicine,* vol. 67, pp. 601-608, Mar 2012.

[25] J. R. Keltner, J. W. Carlson, M. S. Roos, S. T. Wong, T. L. Wong, and T. F. Budinger, "Electromagnetic fields of surface coil in vivo NMR at high frequencies," *Magn Reson Med,* vol. 22, pp. 467-80, Dec 1991.